

# Enhanced Production of Neutral and Ionic Fragments of Core-Excited Molecules

*State-specific fragmentation dynamics for excited and ionic fragments of gaseous and condensed  $\text{Si}(\text{CH}_3)_2\text{Cl}_2$  following Cl 2p and Si 2p core-level excitations have been characterized. The Cl 2p  $\rightarrow 15a_1^*$  excitation of  $\text{Si}(\text{CH}_3)_2\text{Cl}_2$  induces significant enhancement of the  $\text{Cl}^+$  desorption yield in the condensed phase and the  $\text{Si}(\text{CH}_3)_2^+$  and  $\text{SiCH}_3^+$  yields in the gaseous phase. The core-to-Rydberg excitations at both Si 2p and Cl 2p edges lead to enhanced production of the excited fragments. These complementary results provide deeper insight into the origin of state-selective fragmentation of molecules via core-level excitation*

X-ray induced molecular photolysis on surfaces has recently received growing attention, because the understanding of such chemistry is essential for the development of microelectronic devices in the nanometer range. In addition, detailed investigations of ion desorption of molecules occurred on surfaces by inner-shell excitation are considerably valuable for the following fields: (a) vacuum technology to suppress ion desorption produced by electron or photon impact; (b) chemical reactions induced by high-energy particles on interstellar dust, inner-wall of accelerators, and fusion reactor; and (c) radiation damage of biomolecules and X-ray optics.

With synchrotron radiation of tunable energy, one can prepare the molecule in a well defined core-excited state and investigate the associated electronic relaxation channels and fragmentation pathways. An intriguing subject in surface photochemistry is the selective photoexcitation and subsequent cleavage of a specific chemical bond in the adsorbed molecule by tuning the photon energy to a particular absorption resonance. The site-specific fragmentation via core-level excitation was identified in several systems, but was not observed in some molecules, such as  $\text{Fe}(\text{CO})_2(\text{NO})_2$ . The complex relaxation processes for site-selective fragmentation of core-excited molecules are not fully understood and remain the subject of extensive research.

It is known that the photodesorption yield of neutral products for molecular adsorbates on surfaces via photoexcitation is much higher than that of ions, because reneutralization process plays an important role in photon stimulated ion desorption. However, the detection of neutral products or transient species is more difficult than of ions. For the gas phase, such measurements are difficult because of the low density of gaseous molecules and the inefficiency of detectors for neutrals. The investigation of the dissociation dynamics of neutral fragments of gaseous-phase molecules and molecular

adsorbates on surfaces following core-level excitation is a promising field due to the complexity of the new physical processes involved in molecular dissociation.

On the solid surface, the dissociation dynamics of core-excited molecules can be strongly modified as compared with the gaseous phase due to electronic interaction with the substrate and/or neighbouring molecules. In order to obtain profound insight to the complex relaxation processes of molecular adsorbates on surfaces following inner-shell photoexcitation, coordinated studies of gaseous-phase molecules and solid-state analogues using various experimental techniques are indispensable.

In the present study, we investigated the mechanism of state-selective dissociation processes of excited fragments for gaseous  $\text{Si}(\text{CH}_3)_2\text{Cl}_2$  following the Cl 2p and Si 2p core-level excitations to various resonances by combining photon-stimulated ion dissociation, x-ray absorption, resonant photoemission, ion kinetic energy distribution, and dispersed UV/optical fluorescence measurements.

Figures 1(a) and 1(b) show fragmented ion yields following Cl 2p core-level excitation for condensed and gaseous  $\text{Si}(\text{CH}_3)_2\text{Cl}_2$ , respectively, with the Cl  $L_{23}$ -edge x-ray absorption spectrum for comparison. The absorption peaks labeled 1, 1' and 2, 2' in Fig. 1 are ascribed to the Cl 2p  $\rightarrow 15a_1^*$  (Si-Cl) antibonding orbital and Cl 2p  $\rightarrow 10b_1^*$  (Si-Cl) antibonding orbital transitions, respectively. Excitations to Rydberg orbitals are responsible for the absorption peaks labeled 3, 3'. The broad band marked 4 is attributed to the shape resonance. As shown in Fig. 1(a), the photon stimulated ion desorption (PSID) spectra of  $\text{H}^+$ ,  $\text{CH}_3^+$ ,  $\text{SiCl}^+$ , and  $\text{Si}(\text{CH}_3)_2\text{Cl}^+$  follow the Cl  $L_{23}$ -edge total-electron yield (TEY) photoabsorption curve of solid  $\text{Si}(\text{CH}_3)_2\text{Cl}_2$ . In contrast, a significant dissimilarity of the  $\text{Cl}^+$  PSID spectrum and the Cl  $L_{23}$ -edge TEY spectrum of condensed  $\text{Si}(\text{CH}_3)_2\text{Cl}_2$  is observed. The  $\text{Cl}^+$  desorption yield shows significant enhancement following the Cl 2p  $\rightarrow 15a_1^*$  excitation when compared

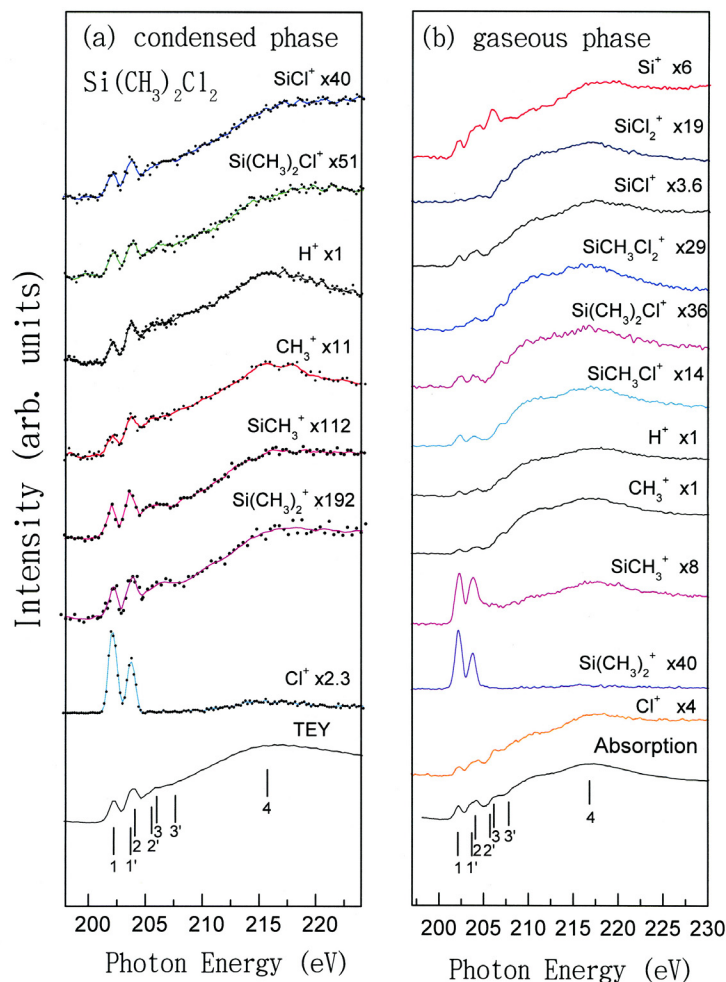


**Fig. 1:** (a) PSID spectra of condensed  $\text{Si}(\text{CH}_3)_2\text{Cl}_2$  via Cl 2p core-level excitation along with Cl 2p-edge TEY spectrum (b) photon-energy dependence of various fragmented ions of gaseous  $\text{Si}(\text{CH}_3)_2\text{Cl}_2$  at the Cl 2p edge together with photoabsorption spectrum.

to the excitations of  $\text{Cl } 2p \rightarrow 10b_1^*$  and  $\text{Cl } 2p \rightarrow$  shape resonance. Besides, the  $\text{Cl } 2p \rightarrow 15a_1^*$  excitation effects a slightly enhanced production of  $\text{SiCH}_3^+$  and  $\text{Si}(\text{CH}_3)_2^+$ , as compared to excitations to Rydberg orbitals.

As demonstrated in Fig. 1(b), the dependency between photon-energy and various fragmented ion yields, except  $\text{Si}(\text{CH}_3)_2^+$ ,  $\text{SiCH}_3^+$ , and  $\text{Si}^+$ , of gaseous  $\text{Si}(\text{CH}_3)_2\text{Cl}_2$  resembles the Cl  $L_{23}$ -edge photoabsorption spectrum. Especially noteworthy is that the  $\text{Cl } 2p \rightarrow 15a_1^*$  excitation of gaseous  $\text{Si}(\text{CH}_3)_2\text{Cl}_2$  generates significant enhancement of  $\text{Si}(\text{CH}_3)_2^+$  and  $\text{SiCH}_3^+$  yields, but little improvement the  $\text{Cl}^+$  yield, as opposed to the condensed phase. Comparison of the  $\text{Si}^+$  yield spectrum and the Cl  $L_{23}$ -edge absorption spectrum in Fig. 1(b) shows that Rydberg excitation produces enhancement of the  $\text{Si}^+$  yield. It is clearly demonstrated from Fig. 1 that there are significant differences in the efficiency for producing fragmented ions, even when these transitions arise from the same atomic site. Hence the character of bound terminating orbital plays a vital role in determining the photodissociation processes. The ion desorption channels for the condensed phase differ notably from the ion dissociation pathways for the gaseous phase. Accordingly, the comparative studies are clearly imperative for elucidating the detailed photofragmentation dynamics of molecular adsorbates on surfaces.

There is a general consensus that, depending on the electronic configuration of the core-excited state, electronic decay of the different core-excited states leads to different ion fragmentation channels. In order to understand the de-excitation processes after resonant excitations of Cl 2p electrons and Si 2p electrons to various empty orbitals, the resonant photoemission spectra of gaseous  $\text{Si}(\text{CH}_3)_2\text{Cl}_2$  were measured by various excitation energies around the Cl 2p and Si 2p absorption edges. The electronic decay processes of molecules following excitation of a core electron to an empty orbital can occur in two principal ways. The excited electron can either remain as a spectator or take part in the decay process. The former process is called a spectator Auger transition and the latter is a participator Auger transition. The participator Auger process leads to the final electronic configuration of one-hole (1h) state which is identical with the direct valence-band photoemission process. In spectator Auger process, the core hole is filled by an Auger-type transition. This process results in a two-hole, one-electron (2h1e) final state, in which two holes are produced in valence orbitals and one electron is excited into an antibonding valence orbital or a Rydberg orbital. The spectator Auger transition should change the structure of the photoelectron spectrum by several eV below the valence band.

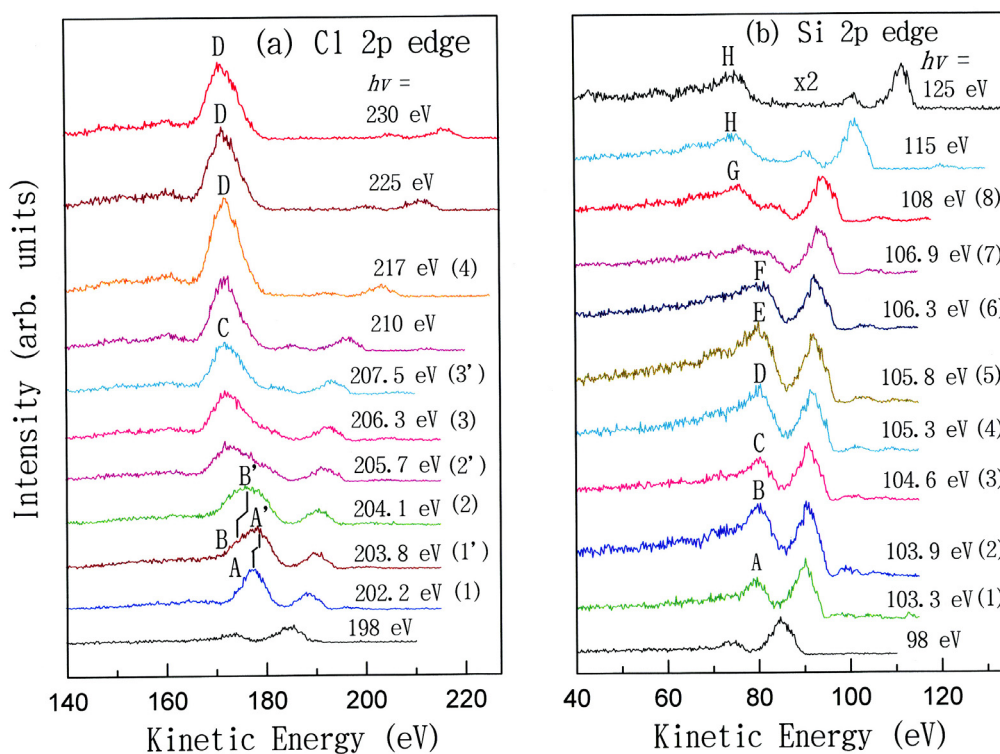


**Fig. 2:** Resonant photoemission spectra of gaseous  $\text{Si}(\text{CH}_3)_2\text{Cl}_2$  excited by various photon energies near the (a) Cl 2p edge and (b) Si 2p edge. The photon energy used for excitation is indicated in each spectrum. The number indicated in each spectrum corresponds to an absorption peak marked in the absorption spectrum in Fig. 1.

In Fig. 2(a) and 2(b), the photoemission spectra of gaseous  $\text{Si}(\text{CH}_3)_2\text{Cl}_2$  excited by various photon energies in the vicinity of Cl 2p and Si 2p absorption edges were reproduced, respectively. The kinetic energy scale in Fig. 2 has as reference to the vacuum level. The photoemission spectra measured at 198-eV and 98-eV photons depict the direct valence-band photoemission peaks in the low binding energy regime, while the spectra excited by the photon energies of 230 eV and 125 eV represent the combinations of Cl LVV and Si LVV normal Auger features, respectively, and the valence-band photoemission peaks.

The photoemission peaks labeled A, A', B, B' and C in Fig. 2(a) are attributed to spectator Auger peaks, whereas feature D corresponds to the normal Auger peak. As noted from Fig. 2(a), with increasing excitation energy, the shift of the spectator Auger peaks increases with reference to the two-hole final states induced by the normal Auger transition. The most striking feature in Fig. 2(a) is the pronounced intensity of the spectator Auger peaks labeled A, A', B, B' and C, when the photon energies vary through the core-to-valence and core-to-Rydberg resonances. This result reveals that the spectator Auger transitions are the dominant decay processes following Cl 2p core-to-valence and Cl 2p core-to-Rydberg excitations, which produce two-hole, one-electron (2h1e) states. In contrast, the shape-resonance excitation was followed by the normal Auger decay. As noted from Fig. 2(a), the spectator Auger peaks via core-to-valence

spectator Auger peaks via core-to-valence excitation have two components. The spectator Auger peaks marked A, A' and B, B' correspond to the spectator Auger transitions following the Cl 2p  $\rightarrow$   $15a_1^*$  and Cl 2p  $\rightarrow$   $10b_1^*$  excitations, respectively. This infers that the spectator electron is localized at the respective valence orbital during the Auger decay.

Following Si 2p core-to-valence and Si 2p core-to-Rydberg excitations, the excited  $\text{Si}(\text{CH}_3)_2\text{Cl}_2$  will decay primarily by the spectator Auger transitions, generating the 2h1e states. Evidence for the predominance of the spectator Auger processes can be observed from the pronounced intensity of spectator Auger peaks labeled A-G in Fig. 2(b) particularly for the photon energies at 103.9, 105.3, and 105.8 eV. In contrast, the excitation at 115 eV was followed by the normal Auger transition with a constant kinetic energy (peak H).

The ion kinetic-energy distribution for an adsorbate on a surface via core-level excitation is related to the steepness of the potential energy curves of the precursor core-excited states or the electronically relaxed states. In Fig. 3, the  $\text{Cl}^+$  kinetic energy distributions of condensed  $\text{Si}(\text{CH}_3)_2\text{Cl}_2$  following Cl 2p core-level excitation are reproduced. As noted, the  $\text{Cl}^+$  ion energy distribution via the excitation Cl 2p  $\rightarrow$   $15a_1^*$  is shifted to greater energy ( $\sim$  0.3 eV) compared to that following the excitations Cl 2p  $\rightarrow$   $10b_1^*$  and Cl 2p  $\rightarrow$  shape resonance. Due to smaller rates of ion reneutralization, the greater  $\text{Cl}^+$  kinetic

energy at the  $\text{Cl}(2p)^{-1}15a_1^*$  resonance of condensed  $\text{Si}(\text{CH}_3)_2\text{Cl}_2$  leads to significant enhancement of  $\text{Cl}^+$  desorption yield. Because  $\text{Si}(\text{CH}_3)_2^+$  and  $\text{SiCH}_3^+$  are massive than  $\text{Cl}^+$ , the slower departure speed of  $\text{Si}(\text{CH}_3)_2^+$  and  $\text{SiCH}_3^+$  from the surface and rapid ion reneutralization greatly diminish the ion yield. Unlike the  $\text{Cl}^+$  spectrum, the  $\text{Cl } 2p \rightarrow 15a_1^*$  excitation of condensed  $\text{Si}(\text{CH}_3)_2\text{Cl}_2$  leads to only a slight enhancement of the  $\text{Si}(\text{CH}_3)_2^+$  and  $\text{SiCH}_3^+$  yields. In the gaseous phase, the ion reneutralization rate is much smaller. As a result, the  $\text{Cl } 2p \rightarrow 15a_1^*$  excitation of gaseous  $\text{Si}(\text{CH}_3)_2\text{Cl}_2$  induces a substantially enhanced production of  $\text{Si}(\text{CH}_3)_2^+$  and  $\text{SiCH}_3^+$ , and presumably neutral Cl radicals. Besides, excitations of Si 2p to the  $15a_1^*$  state of gaseous  $\text{Si}(\text{CH}_3)_2\text{Cl}_2$  also produce significant enhancement of  $\text{Si}(\text{CH}_3)_2^+$  and  $\text{SiCH}_3^+$  yields. After spectator Auger decay of resonant Si 2p and Cl 2p core-excited states of gaseous  $\text{Si}(\text{CH}_3)_2\text{Cl}_2$ , the subsequent electronically relaxed  $2h1e$  final states with a spectator electron localized in a strong antibonding orbital lead to significant enhancement of specific ion fragments. A similar phenomenon was found for  $\text{Si}(\text{CH}_3)_{4-n}\text{Cl}_n$  ( $n = 1, 3$ ),  $\text{SiHCH}_3\text{Cl}_2$  (Si 2p and Cl 2p edges), *etc.*

In Fig. 4(a), the dispersed fluorescence spectra of gaseous  $\text{Si}(\text{CH}_3)_2\text{Cl}_2$  obtained from excitation by various photon energies are displayed. The sharp peaks between 200 and 300 nm are due to emission from excited Si atoms. The emission peak at 431 nm is identified as the CH(A-X) (0,0) band. The 656-nm peak corresponds to the  $\text{H}(n = 3) \rightarrow \text{H}(n = 2)$  transition. The 390-nm peak is ascribed to overlapping emission of excited  $\text{Si}^+$  and CH fragments.

Some emission features are due to a second-order light contribution, as indicated in Fig. 4(a).

Figure 4(b) and 4(c) show yields of the most intense excited fluorescing fragments observed in Fig. 4(a) following Cl 2p and Si 2p core-level excitations, respectively. For comparison, the Cl 2p and Si 2p edges absorption spectra and total fluorescence yield spectra of gaseous  $\text{Si}(\text{CH}_3)_2\text{Cl}_2$  are plotted in Fig. 4(b) and 4(c), respectively. As noted from Fig. 4(b) and 4(c), the excitation spectra of various excited fluorescing fragments and total fluorescence yield spectra differ significantly from the corresponding photoabsorption spectrum. Excitations to Rydberg orbitals from both Si 2p and Cl 2p core levels lead to a noteworthy production of excited atomic fragments, neutral and ionic ( $\text{Si}^*$ ,  $\text{Si}^{+*}$ ), and excited diatomic fragments ( $\text{CH}^*$ ). In particular, the excited neutral atomic fragments  $\text{Si}^*$  are significantly reinforced. This result indicates that, after spectator Auger decay of resonant core-excited molecules, the subsequent  $2h1e$  states with an excited Rydberg electron, as opposed to an excited valence electron, are more likely to dissociate into excited-state fragments. This is due to the fact that the wave function of a diffuse Rydberg electron has less overlap with the molecular-ion core and consequently the  $2h1e$  states dissociate to produce the excited-state fragments before the excited Rydberg electron relax. A similar phenomenon was found for  $\text{Si}(\text{CH}_3)_{4-n}\text{Cl}_n$  ( $n = 1, 3, 4$ ) (Si 2p and Cl 2p edges),  $\text{CH}_{4-n}\text{Cl}_n$  ( $n = 2 - 4$ ) (Cl 2p edge), *etc.* Thus, this finding seems to be of general nature.

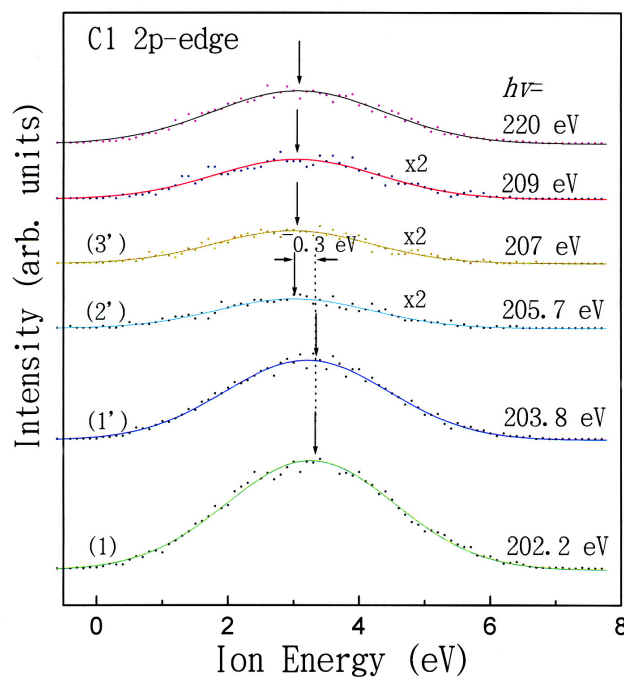


**Fig. 3:**  $\text{Cl}^+$  kinetic energy distributions of condensed  $\text{Si}(\text{CH}_3)_2\text{Cl}_2$  following Cl 2p core-level excitation. The photon energy used for excitation is indicated in each spectrum. The number indicated in each spectrum corresponds to an absorption peak marked in the TEY spectrum in Fig. 1(a).

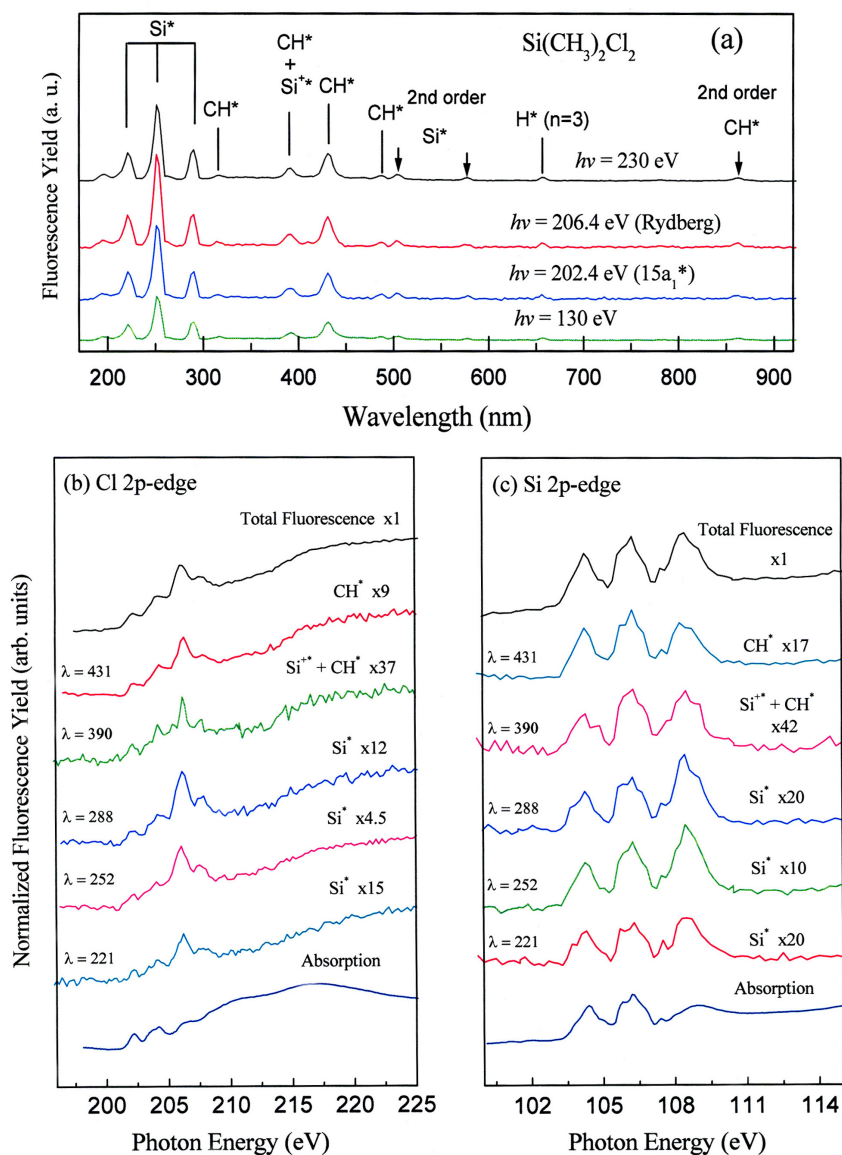


**Fig. 4:** (a) Dispersed fluorescence spectra of gaseous  $\text{Si}(\text{CH}_3)_2\text{Cl}_2$  following excitation by 130-eV, 202.4-eV, 206.6-eV, and 230-eV photons. Photon-energy dependence of various excited fluorescing fragments and total fluorescence yield at the (b) Cl 2p edge and (c) Si 2p edge with the corresponding x-ray absorption spectrum.

In conclusion, the complementary results of gaseous and condensed  $\text{Si}(\text{CH}_3)_2\text{Cl}_2$  obtained by various detection techniques shed new light on the process of selective bond breaking of molecules via core-level excitation.

#### BEAMLINE

09A U5 Spectroscopy beamline  
20A High Energy SGM beamline

#### EXPERIMENTAL STATION

Surface photochemistry end station and effusion-beam end station

#### AUTHORS

J. M. Chen and K. T. Lu  
National Synchrotron Radiation Research Center,  
Hsinchu, Taiwan

#### PUBLICATIONS

- J. M. Chen, K. T. Lu, J. M. Lee, C. I. Ma, and Y. Y. Lee, *Phys. Rev. Letters* **92**, 243002 (2004).
- J. M. Chen, K. T. Lu, and J. M. Lee, *J. Chem. Phys.* **118**, 5087 (2003).

#### CONTACT E-MAIL

[jmchen@nsrrc.org.tw](mailto:jmchen@nsrrc.org.tw)